Korean J. Chem. Eng., 37(11), 2075-2083 (2020)
DOI: 10.1007/s11814-020-0620-4

pISSN: 0256-1115
eISSN: 1975-7220

Fracture toughness enhancement of epoxy resin reinforced with graphene nanoplatelets and carbon nanotubes

Shan-Shan Yao*, Chun-Liu Ma, Fan-Long Jin*,†, and Soo-Jin Park***,†**

*Department of Polymer Materials, Jilin Institute of Chemical Technology, Jilin City 132022, P. R. China
**Changchun Hyperions Scientific Co., Ltd., Changchun City 130000, P. R. China
***Department of Chemistry, Inha University, Nam-gu, Incheon 22212, Korea
(*Received 22 March 2020 • Revised 13 June 2020 • Accepted 30 June 2020*)

Abstract−Graphene nanoplatelets (GNPs)/silane-coupling-agent-treated GNPs (KH- GNPs) and hydroxyl multi-walled carbon nanotubes (MWCNTs-OH) were added as reinforcing agents to an epoxy matrix, diglycidylether of bisphenol-A (DGEBA), to improve the fracture toughness of DGEBA. The influence of the MWCNT-OH fraction on the thermal and flexural properties, fracture toughness, and morphology of the DGEBA/GNP/MWCNT-OH and DGEBA/KH-GNP/MWCNT-OH nanocomposites was investigated. The results indicate that the fracture toughness of the DGEBA/KH-GNP/MWCNT-OH nanocomposites increased from 1.09 to 1.46 MPa·m$^{1/2}$, which is 33.9% greater than that of pristine DGEBA. Analysis of the fracture surfaces of the nanocomposites showed a rough morphology with numerous tortuous and river-like structures. In addition, the MWCNTs-OH were slightly pulled out or broken in the epoxy matrix during the fracture toughness tests.

Keywords: Epoxy Resin, Graphene Nanoplatelets, Carbon Nanotubes, Flexural Properties, Fracture Toughness

INTRODUCTION

Epoxy resin is one of the most industrially important thermosetting polymers. The most widely used epoxy resin is an aromatic type, diglycidylether of bisphenol-A (DGEBA). Cured DGEBA epoxy resin exhibits excellent mechanical properties, good chemical resistance, and excellent thermal stability, which has led to its widespread use in adhesives, coatings, electronics, automobiles, matrix materials, and aerospace applications. However, cured DGEBA epoxy resin exhibits poor crack resistance and brittle fracture because of its high cross-linking density, which limits its broader application [1-9].

Epoxy resin is often modified by the dispersion of rubbers, thermoplastic resins, and inorganic fillers; in addition, solution mixing, melt blending, and in situ polymerization are widely used to modify epoxy resin. Among these approaches, the incorporation of various fillers is important to improving the fracture toughness of epoxy resins. Compared with microfillers, nanofillers have been more widely used in the preparation of epoxy-based composites because of their large specific surface area and strong interaction with the epoxy matrix [10-14].

Graphene nanoplatelets (GNPs) and carbon nanotubes (CNTs) are two excellent carbon nanomaterials among carbon-based filler materials. They exhibit comprehensive and excellent performance, including excellent chemical stability and good mechanical, electrical, and thermal properties, which have led to their widespread use to strengthen and toughen epoxy-based materials [15-17]. However, poor dispersibility and low interfacial adhesion of nanofillers in polymer matrixes adversely affect the mechanical properties of the resulting composites. To improve the dispersibility and interfacial adhesion of nanofillers, researchers use various surface modification methods, including both chemical and physical methods. In addition, combining two nanofillers to prepare polymer-based hybrid nanocomposites not only makes good use of the advantages of the individual fillers, but can also lead to a synergistic effect between the two nanofillers [18-26].

Several researchers have studied the effect of GNPs and multi-walled CNTs (MWCNTs) on the mechanical, thermal, and electric properties of epoxy-based composites. Han et al. [27] investigated the mechanical properties of GNPs and MWCNTs reinforced epoxy adhesives. Their results indicated that the Young's modulus, lap shear strength, and energy release rate increased by 80%, 25%, and 231% at 0.5 vol% MWCNTs, respectively, while these same properties increased by 68%, 22%, and 195% at 0.5 vol% GNPs, respectively. Zakaria et al. [28] compared the mechanical, thermal, and dielectric properties of GNPs and MWCNTs filled epoxy nanocomposites. Their experimental results showed that the flexural strength, thermal conductivity, and dielectric constant of GNPs filled epoxy nanocomposites improved by up to 17%, 126%, and 171%, respectively, while MWCNTs filled epoxy nanocomposites improved by up to 29%, 60%, and 73%, respectively. Cha et al. [29] studied the mechanical properties of epoxy nanocomposites reinforced by melamine-functionalized GNPs and MWCNTs. Their results indicated that the fracture toughness of the nanocomposite increased by 95% with 2 wt% melamine-functionalized MWCNTs and by 124% with 2 wt% melamine-functionalized GNPs. Chang et al. [30] prepared GNP/MWCNT/epoxy nanocomposites using supercritical carbon dioxide. The experimental results demonstrated a syn-

†To whom correspondence should be addressed.
E-mail: jinfanlong@163.com, sjpark@inha.ac.kr

ergistic effect between the GNPs and MWCNTs with a 68 and 190% increase in the thermal conductivity of GNP/MWCNT/epoxy nanocomposite over the individual GNP/epoxy and MWCNT/epoxy nanocomposites, respectively, after applying supercritical carbon dioxide mixing. Rao et al. [18] investigated the synergy between GNPs and MWCNTs on the shear properties of epoxy adhesive. The results demonstrated a clear synergistic effect for 0.75 wt% MWCNTs/GNPs hybrid nanocomposites as they yielded the highest enhancement of shear strength and elongation by 36.6% and 33.2%, respectively, compared with pristine epoxy adhesive.

In our previous work, we studied the surface modification of GNPs (KH-GNPs) using a silane coupling agent and investigated the influence of the GNP/KH-GNP fraction on the thermal stability and mechanical properties of DGEBA/GNP and DGEBA/KH-GNP nanocomposites [31]. In the present study, DGEBA/GNP/carboxyl functionalized MWCNT (MWCNT-OH) and DGEBA/KH-GNP/MWCNT-OH nanocomposites were prepared via solution blending using DGEBA as a polymer matrix and GNPs/KH-GNPs and MWCNTs-OH as reinforcing agents. The influence of the MWCNT-OH fraction on the thermal and flexural properties, fracture toughness, and morphology of the nanocomposites was studied by thermogravimetric analysis (TGA), thermomechanical analysis (TMA), mechanical testing, Izod impact testing, and field-emission scanning electron microscopy (FE-SEM).

EXPERIMENTAL

1. Materials

The epoxy resin DGEBA (epoxy equivalent weight of 184-195 g/mol, supplied by Nantong Xingchen Synthetic Material Co., Ltd.) was used as the polymer matrix in the present study. 4,4-Diaminodiphenyl methane (DDM), which was used as a curing agent, was purchased from Tianjin Haoda Chemical Co., Ltd. GNPs with a carbon content of 97.1 wt% were obtained from Yantai Sinagraphene Co., Ltd. γ-Methacryloxy propyl trimethoxyl silane (KH-570), which was used as a silane coupling agent, was provided by Jinan Xingfeilong Chemical Co., Ltd. MWCNTs-OH with a carboxyl content of 1.23 wt%, a diameter of 20-30 nm, and a length of 20-50 μm were purchased from Chengdu Organic Chemicals Co., Ltd., Chinese Academy of Sciences. Anhydrous ethanol as a solvent was provided by Damao Chemical Reagent Factory.

2. Surface Modification of GNPs

GNPs (1 g) were dispersed in 200 mL of anhydrous ethanol and then ultrasonically treated at 25 °C for 2 h. KH-570 (0.5 g) and 7 mL of water were added to the GNP solution and the resultant mixture was heated to 55 °C for 1.5 h. After the reaction, the mixture was filtered, washed until pH-neutral, dried at 60 °C for 1 h, and ground to obtain KH-570-modified GNPs (denoted as KH-GNPs).

3. Sample Preparation

The GNP/KH-GNP fraction was 0.25 wt% while the MWCNT-OH fraction was varied from 0 to 0.5 wt%. A designed amount of DGEBA, GNPs/KH-GNPs, and MWCNTs-OH was mixed at 70 °C for 30 min and then ultrasonically treated at 70 °C for 30 min. An equivalent ratio of DDM was added to the mixture, and the mixture was stirred at 60 °C for 30 min. The mixture was then evacuated to remove trapped air bubbles and subsequently injected into a mold sprayed with a mold-release agent. The mixture was cured at 130 °C for 1 h. The preparation procedure of the DGEBA/GNP/MWCNT-OH and DGEBA/KH-GNP/MWCNT-OH nanocomposites is shown in Fig. 1.

4. Fourier Transform Infrared (FT-IR)

The surface properties of the GNPs and KH-GNPs were investigated using an FT-IR (Perkin-Elmer Co. Digilab FTS-165) spectrometer.

5. Thermogravimetric Analysis

The thermal stability of the DGEBA/GNP/MWCNT-OH and DGEBA/KH-GNP/MWCNT-OH nanocomposites was characterized by TGA (TA Instruments, Q50) from 30 to 800 °C at a heat-

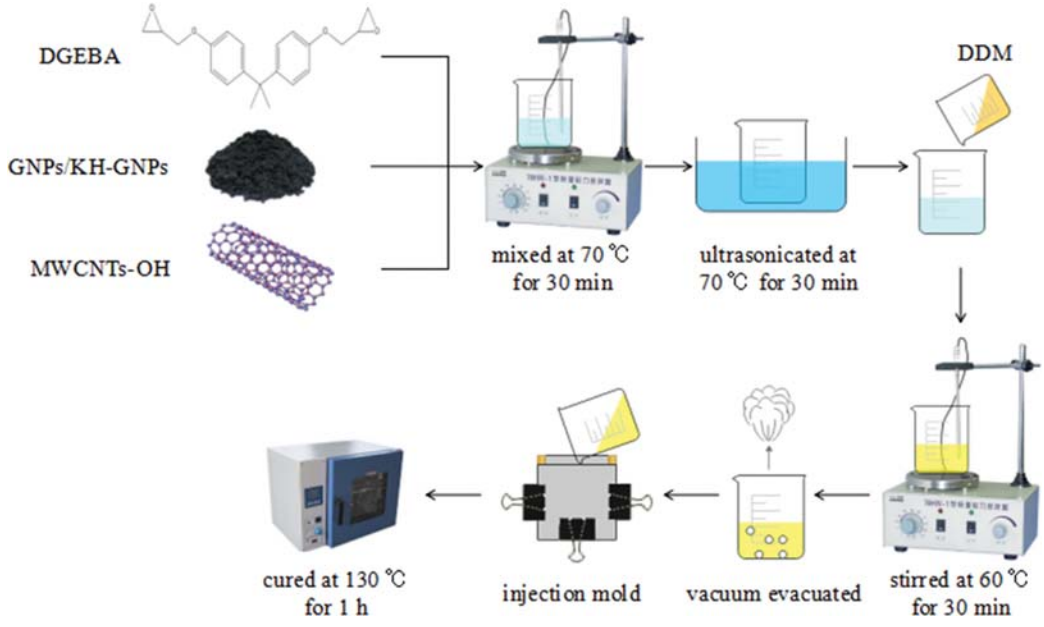

Fig. 1. Schematic illustration of the preparation of DGEBA/GNP/MWCNT-OH and DGEBA/KH-GNP/MWCNT-OH nanocomposites.

ing rate of 10 °C/min under an N_2 flow of 30 mL/min.

6. Thermomechanical Analysis

Thermomechanical properties of the nanocomposites were characterized under an N_2 atmosphere by TMA (TA Instruments, Q400) from 70 to 250 °C at a heating rate of 10 °C/min and under an applied force of 0.05 N.

7. Mechanical Tests

Flexural properties of the nanocomposites were investigated using a mechanical testing apparatus (WDW 3010) according to the methodology specified in standard GB/T 9341-2008.

8. Fracture Toughness Tests

Fracture toughness of the nanocomposites was measured by mechanical testing (WDW 3010) in accordance with the standard method ASTM E399.

9. Impact Strength Tests

Impact strength of the nanocomposites was measured using an Izod impact tester (TP04G-AS1) in accordance with the method described in standard GB/T 1843-2008.

10. Microscopic Morphology Analysis

The fracture surfaces of the nanocomposites after the fracture toughness tests were investigated by FE-SEM (Hitachi, SU 8010).

RESULTS AND DISCUSSION

1. Surface Characteristics of the GNPs

The surface characteristics of the GNPs and KH-GNPs were investigated using FT-IR and TGA. Fig. 2 shows the FT-IR spectra of the GNPs and KH-GNPs. The characteristic absorption peak of the hydroxyl group at 3,432 cm^{-1} decreased after surface modification. Moreover, new peaks corresponding to methyl and methylene groups appeared at 2,927 and 2,855 cm^{-1}, respectively [32].

The silane coupling agent content on the surface of the GNPs was determined using TGA, and the results of weight loss at 900 °C are shown in Table 1. It was found that the silane coupling agent content on the surface of the GNPs was approximately 5.6 wt%. Thus, above results demonstrate that the silane coupling agent was first hydrolyzed in the ethanol solution and then reacted with the hydroxyl groups at the GNP surfaces [31].

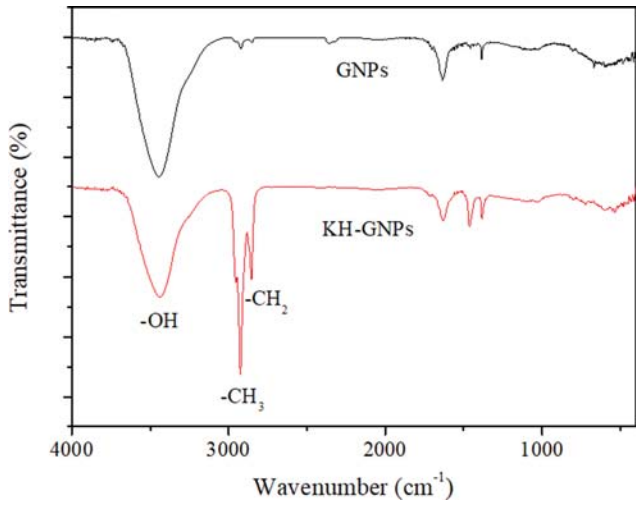

Fig. 2. FT-IR spectra of GNP and KH-GNP.

Table 1. Weight loss at 900 °C for pristine GNPs and KH-GNPs

Sample	GNPs	KH-GNPs
Weight loss at 900 °C (%)	0.59	6.19

2. Thermal Stability

The thermal stability of the DGEBA/GNP/MWCNT-OH and DGEBA/KH-GNP/MWCNT-OH nanocomposites was investigated by TGA; the corresponding TGA thermograms are shown in Fig. 3. Thermal stability factors, such as the decomposition temperature for 5% weight loss ($T_{5\%}$) and the char yield at 800 °C were determined from the TGA thermograms [33,34]; the results are summarized in Table 2.

The $T_{5\%}$ value and char yield at 800 °C of DGEBA increased with the addition of GNPs/KH-GNPs. This result is attributed to the GNPs/KH-GNPs dispersed in the epoxy matrix functioning as a physical barrier to insulate the underlying materials, resulting in increased thermal stability [35]. In contrast, the $T_{5\%}$ value of the DGEBA/GNP/MWCNT-OH and DGEBA/KH-GNP/MWCNT-OH nanocomposites decreased slightly, while the char yield at 800 °C increased slightly with the addition of MWCNTs-OH, indicating

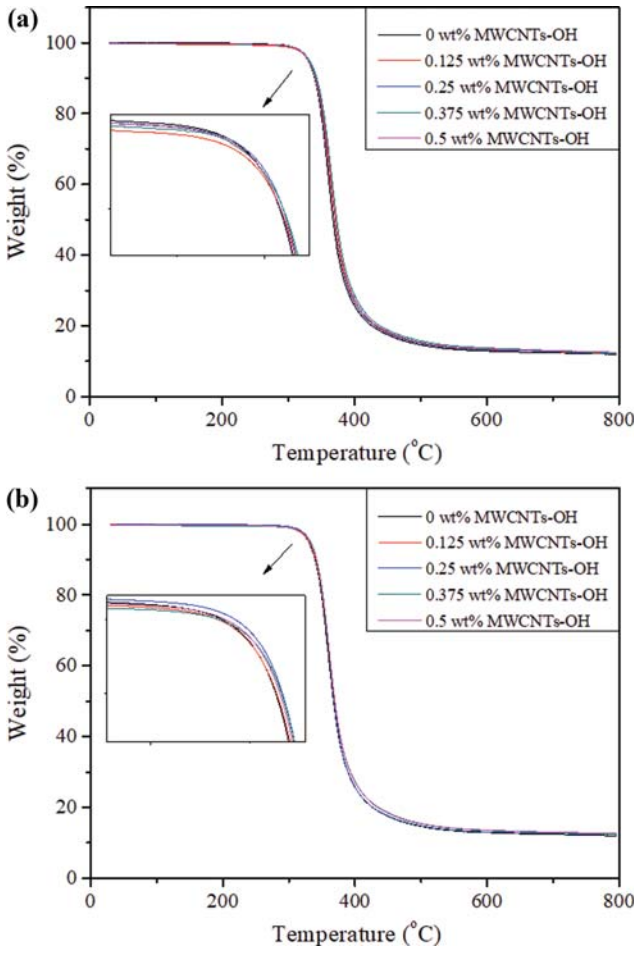

Fig. 3. TGA thermograms of DGEBA/GNP/MWCNT-OH (a) and DGEBA/KH-GNP/MWCNT-OH (b) nanocomposites as a function of MWCNT-OH fraction.

Table 2. Thermal stability factors of DGEBA/GNP/MWCNT-OH and DGEBA/KH-GNP/MWCNT-OH nanocomposites obtained from TGA thermograms

GNP fraction (wt%)	KH-GNP fraction (wt%)	MWCNT-OH fraction (wt%)	$T_{5\%}$ (°C)	Char yield at 800 °C (%)
0	0	0	328.6	11.5
0.25	0	0	334.0	11.9
0.25	0	0.125	331.0	12.1
0.25	0	0.25	332.9	12.7
0.25	0	0.375	331.6	12.2
0.25	0	0.5	330.5	12.6
0	0.25	0	338.9	11.9
0	0.25	0.125	330.6	12.0
0	0.25	0.25	332.8	12.3
0	0.25	0.375	332.6	12.5
0	0.25	0.5	331.8	12.7

that the GNPs and MWCNT-OHs do not have synergistic effect on thermal stability. However, the thermal stability factors at all MWCNT-OH contents were still higher than that of pristine DGEBA.

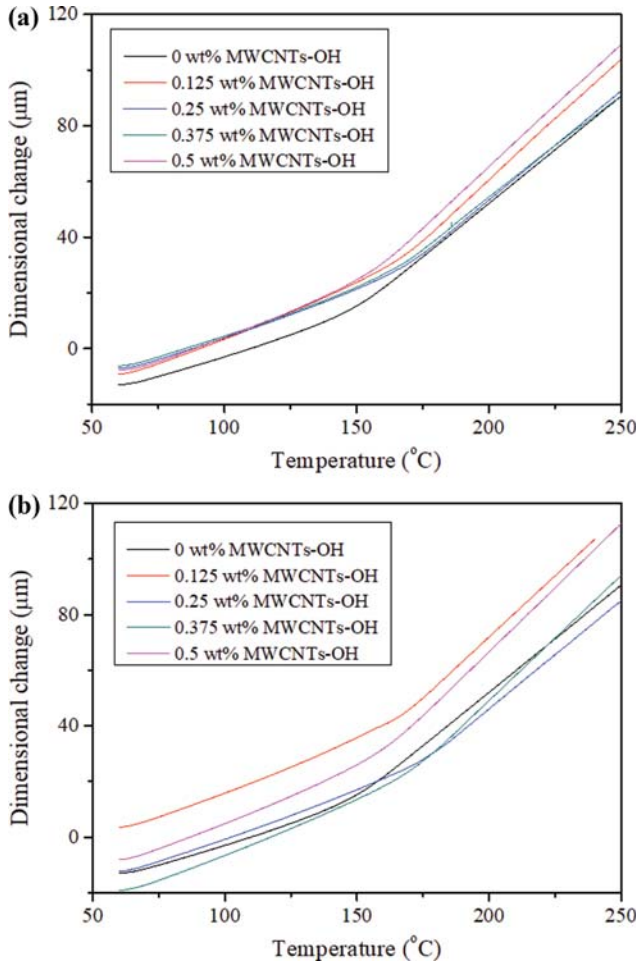

Fig. 4. Dimensional change of DGEBA/GNP/MWCNT-OH (a) and DGEBA/KH-GNP/MWCNT-OH (b) nanocomposites as a function of MWCNT-OH fraction.

These results demonstrate that the thermal stability of DGEBA increased with the addition of GNPs/KH-GNPs and MWCNTs-OH. Rao et al. [18] investigated the thermal stability of epoxy adhesive reinforced with GNPs and MWCNTs. The TGA results showed that the $T_{5\%}$ value of epoxy adhesive with GNPs/MWCNTs hybrids at 0.25-0.75 wt% was higher than that of both pristine epoxy adhesive and epoxy adhesive with either MWCNTs or GNPs, indicating that the MWCNTs and GNPs have a synergistic effect on thermal stability. However, the $T_{5\%}$ value of epoxy adhesive with MWCNTs/GNPs hybrids above 0.75 wt% was lower than that of pristine epoxy adhesive.

3. Thermomechanical Properties

Thermomechanical properties of the DGEBA/GNP/MWCNT-OH and DGEBA/KH-GNP/MWCNT-OH nanocomposites were characterized by TMA; the TMA thermograms are shown in Fig. 4. The glass-transition temperature (T_g) and the coefficient of thermal expansion (CTE) were determined from the TMA thermograms [36], and the results are listed in Table 3.

The T_g value of DGEBA increased from 149.2 to 169.1 and 180.4 °C with the addition of 0.25 wt% GNPs and KH-GNPs, respectively. This result is attributed to the GNPs/KH-GNPs dispersed in the epoxy matrix exhibiting strong adhesion with the epoxy matrix and restricting the mobility of polymer chains at the interface, increasing the T_g of DGEBA [35,37]. By contrast, the T_g of the DGEBA/GNP/MWCNT-OH and DGEBA/KH-GNP/MWCNT-OH nanocomposites decreased with the addition of MWCNTs-OH. However, the T_g of the nanocomposites was still higher than that of pristine DGEBA. Thus, these results demonstrate that the T_g of DGEBA increased with the addition of the GNPs/KH-GNPs and MWCNTs-OH.

The CTE of the DGEBA/GNP/MWCNT-OH and DGEBA/KH-GNP/MWCNT-OH nanocomposites at the glassy region increased with the addition of GNPs/KH-GNPs and MWCNTs-OH. However, the CTE of the nanocomposites at the rubbery region was lower than that of the pristine DGEBA.

4. Flexural Properties

The flexural properties of the DGEBA/GNP/MWCNT-OH and DGEBA/KH-GNP/MWCNT-OH nanocomposites were studied

Table 3. T_g and CTE of DGEBA/GNP/MWCNT-OH and DGEBA/KH-GNP/MWCNT-OH nanocomposites obtained from TMA thermograms

GE content (wt%)	KH-GE content (wt%)	CNT content (wt%)	T_g (°C)	CTE (μm/m·°C)	
				Glassy region	Rubbery region
0	0	0	149.2	69.9	184.7
0.25	0	0	169.1	73.8	174.6
0.25	0	0.125	167.4	74.1	174.2
0.25	0	0.25	167.3	74.2	179.4
0.25	0	0.375	167.3	74.1	170.7
0.25	0	0.5	156.3	72.9	178.9
0	0.25	0	180.4	74.7	167.2
0	0.25	0.125	168.2	77.5	181.3
0	0.25	0.25	175.1	77.2	175.0
0	0.25	0.375	170.8	78.1	178.9
0	0.25	0.5	161.4	75.3	179.9

via flexural strength (σ_f) and elastic modulus (E_b) measurements. The values of the flexural strength and elastic modulus were calculated using the following relationships [38,39]:

$$\sigma_f = \frac{3PL}{2bd^2} \quad (1)$$

$$E_b = \frac{L^3}{4bd^3}\frac{\Delta P}{\Delta m} \quad (2)$$

where P is the applied load (in N), L is the span length (in mm), b is the width of the specimen (in mm), d is the thickness of the specimen (in mm), ΔP is the change in force in the linear portion of the load-deflection curve (in N), and Δm is the corresponding change in deflection (in mm).

Fig. 5 shows the flexural strength of the nanocomposites as a function of the MWCNT-OH fraction. The flexural strength of DGEBA increased from 105.9 to 109.3 MPa (an increase of 3.2%) with the addition of 0.25 wt% GNPs and further increased to 116.8 MPa (an increase of 10.3%) when the MWCNT-OH fraction increased from 0 to 0.25 wt%. This result is attributed to the larger aspect ratio of the MWCNTs-OH and reduced agglomeration of GNPs in the epoxy matrix, which improved the interfacial adhesion between the nanofillers and the epoxy matrix [11,27]. However, when the MWCNT-OH fraction was increased from 0.25 to 0.5 wt%, the magnitude of the improvement in flexural strength decreased from 10.3% to −7.6%. This result is explained as follows: When the MWCNT-OH fraction was added in excess, the nanofillers easily agglomerated in the epoxy matrix and decreased the interfacial adhesion between the nanofillers and the epoxy matrix. This loss of interfacial adhesion led to a lower flexural strength for the DGEBA/GNP/MWCNT-OH nanocomposites [30].

As shown in Fig. 5, the flexural strength of DGEBA increased from 105.9 to 118.3 MPa (an increase of 12.3%) with the addition of 0.25 wt% KH-GNPs, followed by another increased to 125.9 MPa (an increase of 18.9%) when the MWCNT-OH fraction increased from 0 to 0.25 wt%. This behavior is attributed to the surface treatment introducing organic functional groups onto the sur-

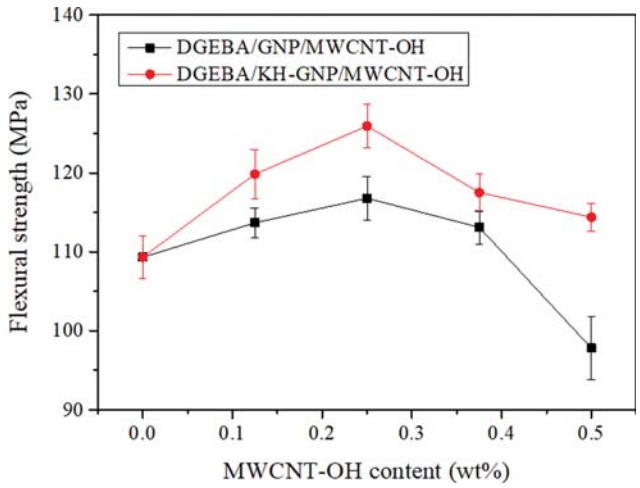

Fig. 5. Flexural strength of DGEBA/GNP/MWCNT-OH and DGEBA/KH-GNP/MWCNT-OH nanocomposites as a function of MWCNT-OH fraction.

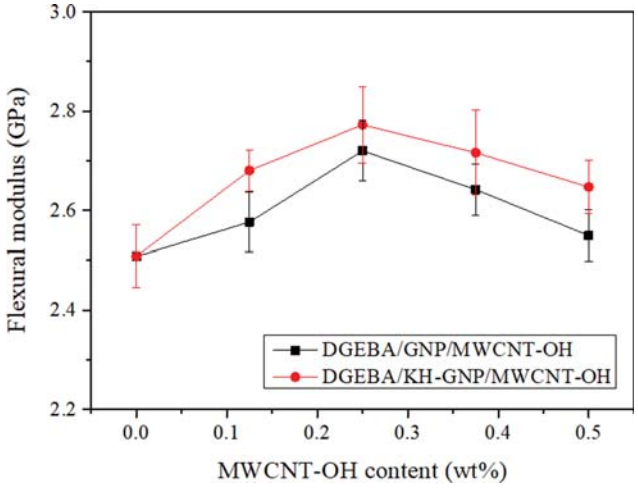

Fig. 6. Elastic modulus of DGEBA/GNP/MWCNT-OH and DGEBA/KH-GNP/MWCNT-OH nanocomposites as a function of MWCNT-OH fraction.

faces of the nanofillers and improving the interfacial adhesion between the nanofillers and the epoxy matrix, increasing the flexural strength of the DGEBA/KH-GNP/MWCNT-OH nanocomposites [31,32]. When the MWCNT-OH fraction was increased from 0.25 to 0.5 wt%, the improvement of flexural strength decreased from 18.9% to 8.1%. However, the flexural strength of the DGEBA/KH-GNP/MWCNT-OH nanocomposite containing 0.5 wt% MWCNTs-OH was still greater than that of the pristine DGEBA.

Fig. 6 shows the elastic modulus of the DGEBA/GNP/MWCNT-OH and DGEBA/KH-GNP/MWCNT-OH nanocomposites as a function of the MWCNT-OH fraction. The elastic modulus of the nanocomposites increased from 2.22 to 2.51 GPa (an increase of 13.1%) and 2.7 GPa (an increase of 21.6%) with the addition of 0.25 wt% GNPs/KH-GNPs and increased to 2.72 GPa (an increase of 22.5%) and 2.77 GPa (an increase of 24.8%) when the MWCNT-OH fraction was increased from 0 to 0.25 wt%, respectively. This result is attributed to the nanofillers dispersed in the epoxy matrix restricting the mobility of polymer chains under the applied load [28]. With increasing MWCNT-OH fraction from 0.25 to 0.5 wt%, the magnitude in the improvement in the elastic modulus of DGEBA/GNP/MWCNT-OH and DGEBA/KH-GNP/MWCNT-OH nanocomposites decreased from 22.5% and 24.8% to 14.9% and 19.4%, respectively. This result indicates that the elastic modulus of the DGEBA/GNP/MWCNT-OH and DGEBA/KH-GNP/MWCNT-OH nanocomposites containing 0.5 wt% MWCNT-OH was greater than that of the pristine DGEBA.

5. Fracture Toughness

The fracture toughness of the DGEBA/GNP/MWCNT-OH and DGEBA/KH-GNP/MWCNT-OH nanocomposites was investigated on the basis of critical stress intensity factor (K_{IC}) measurements. The K_{IC} values were calculated on the basis of the following relationship:

$$K_{IC}=PBW^{1/2}Y \quad (3)$$

where P is the peak load (in kN), B is the specimen thickness (in cm), W is the specimen width (in cm), and Y is the shape factor.

Fig. 7 shows the fracture toughness of the nanocomposites as a function of the MWCNT-OH fraction. The K_{IC} value of DGEBA increased from 1.09 to 1.17 MPa·m$^{1/2}$ (an increase of 7.3%) with the addition of 0.25 wt% GNPs and further increased to 1.32 MPa·m$^{1/2}$ (an increase of 21.1%) when the MWCNT-OH fraction was increased from 0 to 0.25 wt%. The increase in fracture toughness resulted from two main effects: (a) the GNPs dispersed in the epoxy matrix absorbed a large amount of energy through plastic deformation of the matrix, and (b) the MWCNTs-OH exhibited high interfacial adhesion with the epoxy matrix through bonding at the MWCNT-OH-polymer interface [40]. When the MWCNT-OH fraction was increased from 0.25 to 0.5 wt%, the magnitude of the improvement in K_{IC} decreased from 21.1% to 0.9%. This behavior is attributed to the nanofillers in the epoxy matrix readily agglomerating at high MWCNT-OH fractions and therefore likely to concentrate stress, resulting in the deterioration of the fracture toughness of the DGEBA/GNP/MWCNT-OH nanocomposite [41].

As shown in Fig. 7, the K_{IC} value of DGEBA increased from 1.09 to 1.25 MPa·m$^{1/2}$ (an increase of 14.7%) with the addition of 0.25 wt% KH-GNP, followed by another increase to 1.46 MPa·m$^{1/2}$ (an increase of 33.9%) when the MWCNT-OH fraction was increased from 0 to 0.25 wt%. This behavior is attributed to the surface treatment increasing the dispersion of the nanofillers in the epoxy matrix, which in turn increased the interfacial adhesion between the nanofillers and the epoxy matrix, resulting in an enhancing of the fracture toughness of the DGEBA/KH-GE/MWCNT-OH nanocomposites [29,37]. This result is also attributable to high interfacial adhesion between the MWCNTs-OH and the epoxy matrix. When the MWCNT-OH fraction was increased from 0.25 to 0.5 wt%, the magnitude of the improvement in K_{IC} decreased from 33.9 to 21.1%. However, the K_{IC} value of the DGEBA/KH-GNP/MWCNT-OH nanocomposite containing 0.5 wt% MWCNTs-OH was higher than both that of the pristine DGEBA and the DGEBA/KH-GNP nanocomposite. These results demonstrate that the fracture toughness of DGEBA is improved by the addition of KH-GNPs and further enhanced by the addition of MWCNTs-OH.

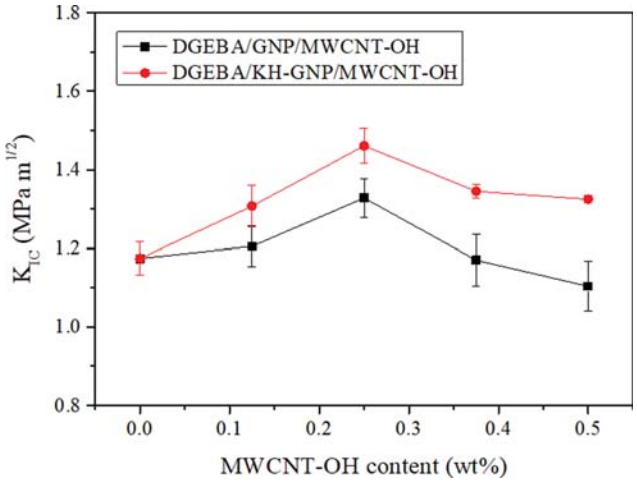

Fig. 7. Fracture toughness of DGEBA/GNP/MWCNT-OH and DGEBA/KH-GNP/MWCNT-OH nanocomposites as a function of MWCNT-OH fraction.

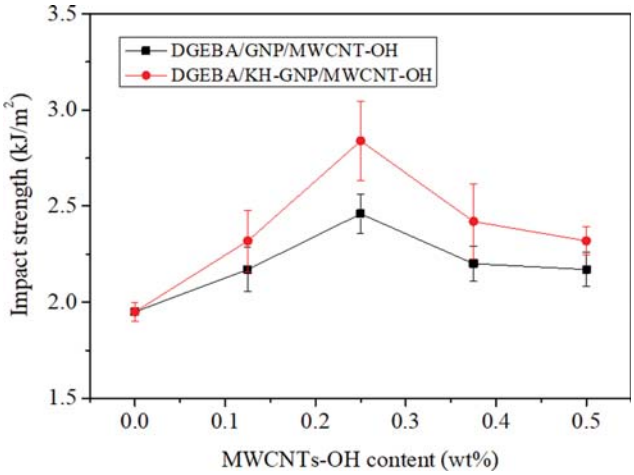

Fig. 8. Impact strength of DGEBA/GNP/MWCNT-OH and DGEBA/KH-GNP/MWCNT-OH nanocomposites as a function of MWCNT-OH fraction.

6. Impact Strength

Fig. 8 shows the impact strength of the DGEBA/GNP/MWCNT-OH and DGEBA/KH-GNP/MWCNT-OH nanocomposites as a function of the MWCNT-OH fraction. The impact strength value of DGEBA increased from 1.75 to 1.95 kJ/m^2 (an increase of 11.4%) with the addition of 0.25 wt% GNPs and further increased to 2.46 kJ/m^2 (an increase of 40.5%) when the MWCNT-OH fraction was increased from 0 to 0.25 wt%. These results can be attributed to the GNPs dispersed in the epoxy matrix that absorbs a large amount of energy and the MWCNTs-OH that exhibited high interfacial adhesion with the epoxy matrix [40].

As shown in Fig. 8, the impact strength value of DGEBA increased from 1.75 to 2.28 kJ/m^2 (an increase of 30.2%) with the addition of 0.25 wt% KH-GNP and further increased to 2.84 kJ/m^2 (an increase of 62.2%) when the MWCNT-OH fraction was increased from 0 to 0.25 wt%. The results are attributed to the surface treatment increasing the interfacial adhesion between the nanofillers and the epoxy matrix, which results in an enhancement of the impact strength of the DGEBA/KH-GNP/MWCNT-OH nanocomposites [29,37].

Several researchers have also studied the effect of GNPs/MWCNTs hybrid on the mechanical properties of epoxy-based composites. Kwon et al. [42] investigated the effect of GNPs/MWCNTs hybrid on the short beam strength of carbon fiber-reinforced epoxy composites. Their results indicated that the short beam strength of GNPs/MWCNTs hybrid-coated carbon fiber/epoxy composites was 10.6% higher than that of carbon fiber/epoxy composites and 2.4% higher than that of GNPs-coated carbon fiber/epoxy composites. Moreover, Rao et al. [18] investigated the shear strength of epoxy adhesive reinforced with GNPs/MWCNTs hybrid. The experimen-

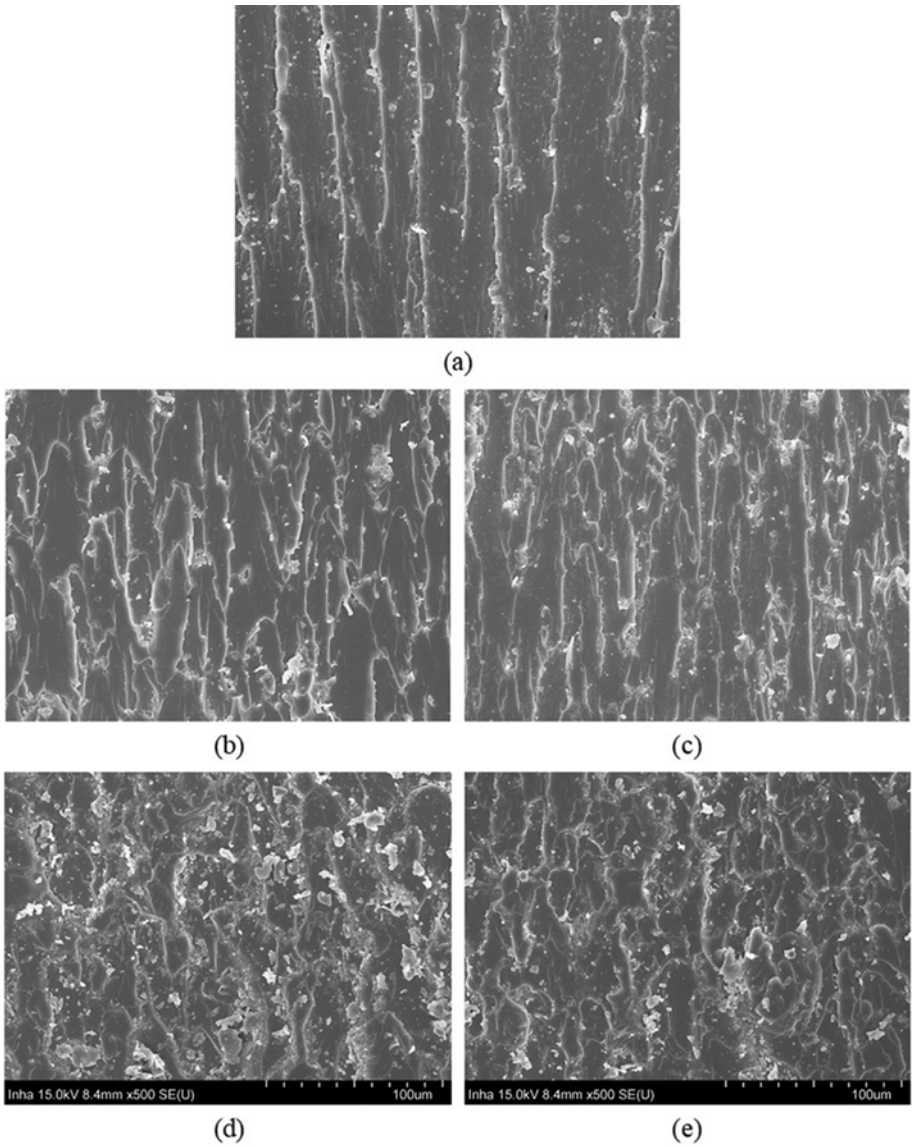

Fig. 9. SEM micrographs of DGEBA/GNP/MWCNT-OH and DGEBA/KH-GNP/MWCNT-OH nanocomposites after the K_{IC} tests: (a) Pristine DGEBA; (b) 0.25 wt% GNPs; (c) 0.25 wt% KH-GNPs; (d) 0.25 wt% GNPs+0.25 wt% MWCNTs-OH; (e) 0.25 wt% KH-GNPs+0.25 wt% MWCNTs-OH (magnification of 500, scale bar of 100 μm).

tal results showed that, based on pristine epoxy adhesive, the shear strength of the epoxy adhesive improved by 19.5% with the addition of GNPs and increased by 36.6% with the incorporation of GNPs/MWCNTs hybrid. The above results demonstrate that the addition of KH-GNPs/MWCNTs-OH hybrid in this study could significantly improve the fracture toughness and impact strength of DGEBA.

7. Morphological Analysis

The fracture toughness behavior of the DGEBA/GNP/MWCNT-OH and DGEBA/KH-GNP/MWCNT-OH nanocomposites was further studied by SEM. Fig. 9 shows SEM images of the fracture surfaces of the nanocomposites after the K_{IC} tests.

As shown in Fig. 9(a), pristine DGEBA exhibits a mirror-like morphology with an ordered crack, accounting for its brittleness [43]. By contrast, SEM images of the DGEBA/GNP and DGEBA/KH-GNP nanocomposites containing 0.25 wt% GNPs/KH-GNPs show a relatively rough morphology with river-like structures, indicating plastic deformation prior to fracture [44] (Fig. 9(b) and (c)). SEM images of the DGEBA/GNP/MWCNT-OH and DGEBA/KH-GNP/MWCNT-OH nanocomposites containing 0.25 wt% MWCNTs-OH also show a rough morphology with numerous tortuous and river-like structures, accounting for their high fracture toughness [45], as shown in Fig. 9(d) and (e).

The dispersion state of the MWCNTs-OH in the DGEBA/KH-GNP/MWCNT-OH nanocomposites was examined by SEM; the corresponding SEM images are shown in Fig. 10. As shown in Fig. 10(a), the MWCNTs-OH are well distributed in the epoxy matrix at low MWCNT-OH fractions. In addition, the MWCNTs-OH are slightly pulled out or broken in the epoxy matrix during the K_{IC} tests, indicating that the MWCNTs-OH exhibit strong interfacial bonding with the epoxy matrix. However, when the MWCNT-OH fraction is excessively high, the MWCNTs-OH aggregate in the epoxy matrix, as shown in Fig. 10(b).

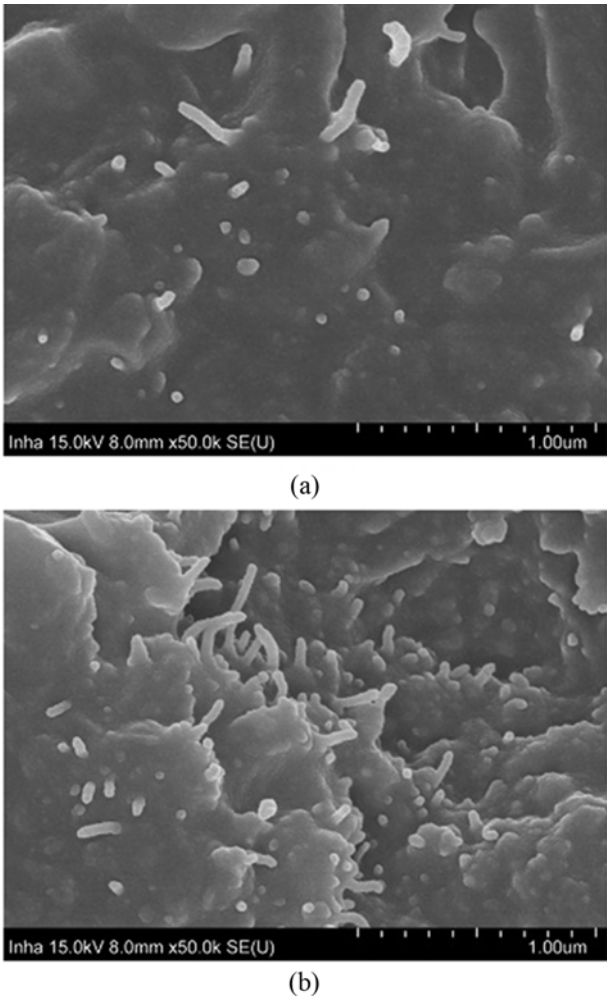

Fig. 10. SEM micrographs of DGEBA/KH-GNP/MWCNT-OH nanocomposites after the K_{IC} tests: (a) Well distributed MWCNTs-OH; (b) aggregated MWCNTs-OH (magnification of 50,000, scale bar of 1 μm).

CONCLUSIONS

The thermal and mechanical properties, fracture toughness, and morphology of DGEBA/GNP/MWCNT-OH and DGEBA/KH-GNP/MWCNT-OH nanocomposites were investigated. The thermal stability and T_g of DGEBA increased with the addition of 0.25 wt% GNPs/KH-GNPs and decreased with increasing MWCNT-OH fraction. The flexural strength, elastic modulus, and fracture toughness of DGEBA increased upon the addition of GNPs/KH-GNPs and further increased as the MWCNT-OH fraction was increased to 0.25 wt%. SEM images of the DGEBA/GNP/MWCNT-OH and DGEBA/KH-GNP/MWCNT-OH nanocomposites show a rough morphology with numerous tortuous and river-like structures. The fracture surfaces of the nanocomposites also show that the MWCNTs-OH were slightly pulled out or broken in the epoxy matrix during the K_{IC} tests. These results suggest that the KH-GNPs and MWCNTs-OH have a synergistic reinforcing effect for improving the fracture toughness of DGEBA without adversely affecting its thermal and mechanical properties.

ACKNOWLEDGEMENTS

This work was supported by the Technology Innovation Program (or Industrial Strategic Technology Development Program (10083586, Development of petroleum based graphite fibers with ultra-high thermal conductivity) funded by the Ministry of Trade, Industry & Energy (MOTIE, Korea) and the Technological Innovation R&D Program (S2829590) funded by the Small and Medium Business Administration (SMBA, Korea).

REFERENCES

1. M. Zhang, M. Chen and Z. Ni, *Polymer*, **186**, 122009 (2020).
2. J. Behin, L. Rajabi, H. Etesami and S. Nikafshar, *Korean J. Chem. Eng.*, **35**, 602 (2018).
3. A. M. Atta, A. O. Ezzat, A. M. El-Saeed, M. H. Wahby and M. M. S. Abdallah, *Prog. Orga. Coat.*, **140**, 105502 (2020).
4. J. Y. Qin, W. C. Zhang and R. J. Yang, *Mater. Design*, **178**, 107834 (2019).
5. P. Wang, H. Xiao, C. Duan, B. Wen and Z. Li, *Polym. Degrad. Stabil.*, **173**, 109078 (2020).

6. M. A. Alam, U. A. Samad, R. Khan, M. Alam and S. M. Al-Zahrani, *Korean J. Chem. Eng.*, **34**, 2301 (2017).
7. C. Chen, Y. He, G. Xiao, F. Zhong and Y. Wu, *Prog. Orga. Coat.*, **139**, 105448 (2020).
8. A. K. Singh, B. P. Panda, S. Mohanty, S. K. Nayak and M. K. Gupta, *Korean J. Chem. Eng.*, **34**, 3028 (2017).
9. G. S. Dhole, G. Gunasekaran, R. Naik, T. Ghorpade and M. Vinjamur, *Prog. Orga. Coat.*, **138**, 105425 (2020).
10. Y. Zhang, L. Li, K. Nie and S. Zheng, *Mater. Chem. Phys.*, **240**, 122183 (2020).
11. A. Bisht, K. Dasgupta and D. Lahiri, *Polym. Test.*, **81**, 106274 (2020).
12. A. Wagih, T. A. Sebaey, A. Yudhanto and G. Lubineau, *Compos. Struct.*, **239**, 112022 (2020).
13. C. L. Chiang, H. Y. Chou and M. Y. Shen, *Compos. Part A-Appl. S.*, **130**, 105718 (2020).
14. X. J. Shen, C. Y. Dang, B. L. Tang, X. H. Yang, X. H. Yang, H. J. Nie, J. J. Lu, T. T. Zhang and K. Friedrich, *Mater. Design*, **185**, 108257 (2020).
15. A. Kumar, K. Sharma and A. R. Dixit, *Mol. Simulat.*, **46**, 136 (2020).
16. A. Kumar, K. Sharma and A. R. Dixit, *J. Mater. Sci.*, **54**, 5992 (2019).
17. A. Kumar, K. Sharma and A. R. Dixit, *J. Mater. Sci.*, **55**, 2682 (2020).
18. J. Peng, C. Huang, C. Cao, E. Saiz, Y. Du, S. Dou, A. P. Tomsia, H. D. Wagner, L. Jiang and Q. Cheng, *Matter*, **2**, 220 (2020).
19. Ö. U. Colak, N. Bahlouli, D. Uzunsoy and C. Francart, *Polym. Test.*, **81**, 106219 (2020).
20. H. Yu, Z. Tong, P. Chen, A. Cai and F. Qin, *Curr. Appl. Phys.*, **20**, 510 (2020).
21. Q. Rao, H. Huang, Z. Ouyang and X. Peng, *Polym. Test.*, **82**, 106299 (2020).
22. V. Datsyuk, S. Trotsenko, G. Trakakis, A. Boden and K. Papagelis, *Polym. Test.*, **82**, 106317 (2020).
23. Y. Xiao, Z. Jin, L. He, S. Ma, C. Wang, X. Mu and L. Song, *Compos. Part B-Eng.*, **182**, 107616 (2020).
24. X. F. Sánchez-Romate, J. Martín, A. Jiménez-Suárez, S. G. Prolongo and A. Ureña, *Polymer*, **190**, 122236 (2020).
25. D. Quan, C. Mischo, L. Binsfeld, A. Ivankovic and N. Murphy, *Compos. Struct.*, **235**, 111767 (2020).
26. Y. C. Shin, W. I. Lee and H. S. Kim, *Compos. Struct.*, **236**, 111808 (2020).
27. S. Han, Q. Meng, S. Araby, T. Liu and M. Demiral, *Compos. Part A-Appl. S.*, **120**, 116 (2019).
28. M. R. Zakaria, M. H. A. Kudus, H. M. Akil and M. Z. M. Thirmizir, *Compos. Part B-Eng.*, **119**, 57 (2017).
29. J. Cha, J. Kim, S. Ryu and S. H. Hong, *Compos. Part B-Eng.*, **162**, 283 (2019).
30. H. P. Chang, H. C. Liu and C. S. Tan, *Polymer*, **75**, 125 (2015).
31. F. L. Jin, C. L. Ma, B. T. Guo and S. J. Park, *Bull. Korean Chem. Soc.*, **40**(11), 991 (2019).
32. F. L. Jin, H. Zhang, S. S. Yao and S. J. Park, *Macromol. Res.*, **26**(3), 211 (2018).
33. S. J. Park, G. Y. Heo and F. L. Jin, *Polym. Eng. Sci.*, **55**(11), 2676 (2015).
34. S. J. Park, G. Y. Heo and F. L. Jin, *Macromol. Res.*, **23**(4), 320 (2015).
35. X. Mi, L. Zhong, F. Wei, L. Zeng, J. Zhang, D. Zhang and T. Xu, *Polym. Test.*, **76**, 473 (2019).
36. F. L. Jin and S. J. Park, *Polym. Degrad. Stabil.*, **97**(11), 2148 (2012).
37. D. Yao, N. Peng and Y. Zheng, *Compos. Sci. Technol.*, **167**, 234 (2018).
38. J. Chen, Q. Z. Zhang, Z. S. Hou, F. L. Jin and S. J. Park, *Bull. Mater. Sci.*, **42**, 153 (2019).
39. J. Chen, Y. J. Dong, F. L. Jin and S. J. Park, *Macromol. Res.*, **27**(1), 10 (2019).
40. B. Ramezanzadeh, M. Shamshiri and M. G. Sari, *Prog. Org. Coat.*, **116**, 7 (2018).
41. D. Quan, D. Carolan, C. Rouge, N. Murphy and A. Ivankovic, *Int. J. Adhes. Adhes.*, **81**, 21 (2018).
42. Y. J. Kwon, Y. Kim, H. Jeon, S. Cho, W. Lee and J. U. Lee, *Compos. Part B-Eng.*, **122**, 23 (2017).
43. F. L. Jin, X. Li and S. J. Park, *J. Ind. Eng. Chem.*, **29**(1), 1 (2015).
44. H. Jin, B. Yang, F. L. Jin and S. J. Park, *J. Ind. Eng. Chem.*, **25**(1), 9 (2015).
45. F. L. Jin, H. C. Liu, B. Yang and S. J. Park, *J. Ind. Eng. Chem.*, **24**(4), 20 (2015).